# Search for $X(1870)$ via the decay $J/\psi \to \omega K^+K^-\eta$

M. Ablikim *et al.*[*]
(BESIII Collaboration)

(Received 14 June 2024; accepted 1 August 2024; published 18 September 2024)

Using a sample of $(10087 \pm 44) \times 10^6$ $J/\psi$ events collected by the BESIII detector at the BEPCII collider, we search for the decay $X(1870) \to K^+K^-\eta$ via the $J/\psi \to \omega K^+K^-\eta$ process for the first time. No significant $X(1870)$ signal is observed. The upper limit on the branching fraction of the decay $J/\psi \to \omega X(1870) \to \omega K^+K^-\eta$ is determined to be $9.55 \times 10^{-7}$ at the 90% confidence level. In addition, the branching faction $B(J/\psi \to \omega K^+K^-\eta)$ is measured to be $(3.33 \pm 0.02(\mathrm{stat}) \pm 0.12(\mathrm{syst})) \times 10^{-4}$.

DOI: 10.1103/PhysRevD.110.052005

## I. INTRODUCTION

Within the framework of the Standard Model, the strong interaction is described by quantum chromodynamics, which predicts the existence of unconventional hadrons, such as glueballs, hybrid states, and multiquark states. The discovery and characterization of such states remain a primary focus in hadron physics. The decays of the $J/\psi$ provide an excellent platform for investigating light hadron spectroscopy and searching for unconventional hadrons. Several resonances in the mass range of 1.8 to 1.9 GeV$/c^2$ have been observed in the $J/\psi$ decays, including the $X(p\bar{p})$ [1–3], $X(1835)$ [4–7], $X(1810)$ [8], and $X(1870)$ [9].

The $X(1870)$ resonance was first observed in the $\pi^+\pi^-\eta$ invariant mass spectrum via the decay of $J/\psi \to \omega\pi^+\pi^-\eta$ [9] with a statistical significance of $7.2\sigma$, based on a sample of $(225.2 \pm 2.8) \times 10^6$ $J/\psi$ events collected by the BESIII experiment. Currently, there is less information available on the $X(1870)$. More experimental efforts are needed to go further. A high-statistics data sample collected with BESIII provides an opportunity to confirm the existence of the $X(1870)$ and obtain more information on the properties of the $X(1870)$. Searching for the $X(1870)$ in the $K^+K^-\eta$ decay mode via $J/\psi \to \omega K^+K^-\eta$ is of interest, which can provide more information on the strange-quark component of the $X(1870)$.

## II. BESIII DETECTOR

The BESIII detector [10–12] records symmetric $e^+e^-$ collisions provided by the Beijing Electron Positron Collider II (BEPCII) storage ring [13] in the center-of-mass energy range from 2.0 to 4.95 GeV, with a peak luminosity of $1.1 \times 10^{33}$ cm$^{-2}$ s$^{-1}$ achieved at $\sqrt{s} = 3.773$ GeV. The cylindrical core of the BESIII detector covers 93% of the full solid angle and consists of a helium-based multilayer drift chamber (MDC), a plastic scintillator time-of-flight system (TOF), and a CsI(Tl) electromagnetic calorimeter (EMC), which are all enclosed in a superconducting solenoidal magnet providing a 1.0 T (0.9 T in 2012) magnetic field. The solenoid is supported by an octagonal flux-return yoke with resistive plate counter muon identification modules interleaved with steel. The charged-particle momentum resolution at 1 GeV$/c$ is 0.5%, and the $dE/dx$ resolution is 6% for electrons from Bhabha scattering. The EMC measures photon energies with a resolution of 2.5% (5%) at 1 GeV in the barrel (end cap) region. The time resolution in the TOF barrel region is 68 ps, while that in the end cap region is 110 ps. The end cap TOF system was upgraded in 2015 using multigap resistive plate chamber technology, providing a time resolution of 60 ps, which benefits 83% of the data used in this analysis [14–16].

## III. DATA SET AND MONTE CARLO SIMULATION

The results reported in this article are based on a sample of $(10087 \pm 44) \times 10^6$ $J/\psi$ events [17] collected by the BESIII detector.

Monte Carlo (MC) simulated data samples produced with a GEANT4-based [18,19] software package, which includes the geometric description of the BESIII detector and the detector response [12,20,21], are used to determine detection efficiencies and estimate backgrounds. To thoroughly investigate potential backgrounds, we utilize an inclusive MC sample comprising 10 billion $J/\psi$ events. The inclusive MC sample includes both the production of the $J/\psi$ resonance and the continuum processes incorporated in KKMC [22,23]. All particle decays are modeled with EvtGen [24] using branching fractions (BFs) either

[*]Full author list given at the end of the article.

taken from the Particle Data Group (PDG) [25], when available, or otherwise estimated with LundCharm [26]. Final-state radiation from charged final-state particles is incorporated using the PHOTOS package [27].

In this study, two exclusive MC samples are employed to determine detection efficiencies. These samples correspond to the decays $J/\psi \to \omega K^+K^-\eta$ and $J/\psi \to \omega X(1870) \to \omega K^+K^-\eta$, each consisting of $1\times10^7$ MC events. The decay $\omega \to \pi^+\pi^-\pi^0$ is simulated using a generator considering its Dalitz plot distribution [28], while other decays are generated with the phase-space model.

## IV. MEASUREMENT OF BRANCHING FRACTION OF $J/\psi \to \omega K^+K^-\eta$

### A. Event selection and background analysis

The decay $J/\psi \to \omega K^+K^-\eta$ is reconstructed with $\omega \to \pi^+\pi^-\pi^0$ and $\eta/\pi^0 \to \gamma\gamma$. The final state consists of $K^+K^-\pi^+\pi^-\gamma\gamma\gamma\gamma$, requiring four charged tracks with a net zero charge. Charged tracks detected in the MDC are required to be within a polar angle ($\theta$) range of $|\cos\theta| < 0.93$, where $\theta$ is defined with respect to the $z$ axis, which is the symmetry axis of the MDC. For each track, the distance of closest approach to the interaction point (IP) must be less than 10 cm along the $z$ axis, $|V_z|$, and less than 1 cm in the transverse plane, $|V_{xy}|$. Particle identification (PID) for charged tracks combines measurements of the energy deposited in the MDC ($\mathrm{d}E/\mathrm{d}x$) and the flight time in the TOF to form likelihoods $\mathcal{L}(h)(h = p, K, \pi)$ for each hadron $h$ hypothesis. Charged tracks with $\mathcal{L}(K) > \mathcal{L}(p)$ and $\mathcal{L}(K) > \mathcal{L}(\pi)$ are identified as kaons, and those with $\mathcal{L}(\pi) > \mathcal{L}(K)$ and $\mathcal{L}(\pi) > \mathcal{L}(p)$ as pions.

Photon candidates are identified using isolated showers in the EMC. The deposited energy of each shower must be more than 25 MeV in the barrel region ($|\cos\theta| < 0.80$) and more than 50 MeV in the end cap region ($0.86 < |\cos\theta| < 0.92$). To exclude showers that originate from charged tracks, the angle subtended by the EMC shower and the position of the closest charged track at the EMC must be greater than 10 degrees as measured from the IP. To suppress electronic noise and showers unrelated to the event, the difference between the EMC time and the event start time is required to be within [0, 700] ns. The number of photon candidates in an event is at least four.

To improve the mass resolution, a kinematic fit is applied under the hypothesis $J/\psi \to K^+K^-\pi^+\pi^-\gamma\gamma\gamma\gamma$, imposing constraints on four-momentum conservation and requiring the invariant mass of one pair of photons to the nominal $\pi^0$ mass, which is called the five-constraint (5C) fit [29]. The 5C kinematic fit loops over all $K^+K^-\pi^+\pi^-\gamma\gamma\gamma\gamma$ combinations and the one with the minimum $\chi^2_{5\mathrm{C}}$ value is retained. To further suppress background contributions and improve the significance of signal, the $\chi^2_{5\mathrm{C}}$ requirement is optimized using a figure of merit [30] defined as $S/\sqrt{S+B}$, where $S$ denotes the number of signal events from MC simulation and $B$ represents the number of background events estimated with $\omega$ and $\eta$ sidebands in the data. The nominal criterion is set as $\chi^2_{5\mathrm{C}} < 80$.

The mass windows for $\omega$ and $\eta$ are set to $3\sigma$ around their respective nominal masses, corresponding to $|M(\pi^+\pi^-\pi^0) - m(\omega)| < 0.02\ \mathrm{GeV}/c^2$ and $|M(\gamma\gamma) - m(\eta)| < 0.02\ \mathrm{GeV}/c^2$, where $m(\omega)$ and $m(\eta)$ are obtained from the PDG [25]. To suppress backgrounds containing $\eta'$, an additional requirement of $|M(\pi^+\pi^-\eta) - m(\eta')| > 0.025\ \mathrm{GeV}/c^2$ is applied.

To investigate potential background contributions, the same selection criteria are applied to an inclusive MC sample of $10\times10^9 J/\psi$ events. The topology analysis of the inclusive MC sample is performed with the generic tool TopoAna [31]. A detailed study indicates that there is no peaking background with both an $\omega$ and an $\eta$. Three main types of background contributions are identified. The first type of background is due to $J/\psi \to \omega K^- K^{*+}$, $\omega \to \pi^0\pi^+\pi^-$, $K^{*+} \to \pi^0 K^+$, with an $\omega$ but no $\eta$. The second type of background is due to $J/\psi \to \pi^-\eta\bar{K}^* K^{*+}$, $\eta \to \gamma\gamma$, $\bar{K}^* \to \pi^+K^-$, $K^{*+} \to \pi^0K^+$, with an $\eta$ but no $\omega$. The third type of background is due to $J/\psi \to \rho^-\bar{K}^*K^{*+}$, $\rho^- \to \pi^0\pi^-$, $\bar{K}^* \to \pi^+K^-$, $K^{*+} \to \pi^0K^+$, without any $\omega$ or any $\eta$. These contributions would be considered in the fitting for signal extraction.

### B. Measurement of branching fraction

Figure 1(a) shows the distribution of $M(\pi^+\pi^-\pi^0)$ versus $M(\gamma\gamma)$. A two-dimensional (2D) maximum likelihood fit is performed on the distribution of $M(\pi^+\pi^-\pi^0)$ versus $M(\gamma\gamma)$ of the accepted candidates for $J/\psi \to K^+K^-\pi^+\pi^-\pi^0\gamma\gamma$ to obtain the signal yield of $J/\psi \to \omega K^+K^-\eta$. The fitting model is constructed as

$$
\begin{aligned}
F(\pi^+\pi^-\pi^0\!:\!\gamma\gamma) &= N_{\mathrm{sig}} \times (F(\pi^+\pi^-\pi^0)^{\omega}_{\mathrm{sig}} \cdot F(\gamma\gamma)^{\eta}_{\mathrm{sig}}) \\
&\quad + N^{\mathrm{non-}\eta}_{\mathrm{bkg}} \times (F(\pi^+\pi^-\pi^0)^{\omega}_{\mathrm{sig}} \cdot F(\gamma\gamma)^{\mathrm{non-}\eta}_{\mathrm{bkg}}) \\
&\quad + N^{\mathrm{non-}\omega}_{\mathrm{bkg}} \times (F(\pi^+\pi^-\pi^0)^{\mathrm{non-}\omega}_{\mathrm{bkg}} \cdot F(\gamma\gamma)^{\eta}_{\mathrm{sig}}) \\
&\quad + N^{\mathrm{non-}\omega\eta}_{\mathrm{bkg}} \times (F(\pi^+\pi^-\pi^0)^{\mathrm{non-}\omega}_{\mathrm{bkg}} \cdot F(\gamma\gamma)^{\mathrm{non-}\eta}_{\mathrm{bkg}}), \qquad (1)
\end{aligned}
$$

where the multiplication sign (i.e., $\times$) represents multiplication in mathematics, while the dot sign (i.e., $\cdot$) denotes the product of different dimensions of probability density functions. The signal shapes for $\omega$ (i.e., $F^{\omega}_{\mathrm{sig}}$) and $\eta$ (i.e., $F^{\eta}_{\mathrm{sig}}$) are modeled with a sum of two Johnson functions [32] sharing the same mean and width parameters. The mean and width parameters for the $\omega$ and $\eta$ are determined from the 2D fits to the data. The tail parameters and fractions of each Johnson function are fixed to the values obtained from the fit to the signal MC events. The background shapes of non-$\omega$ (i.e., $F^{\mathrm{non-}\omega}_{\mathrm{bkg}}$) and non-$\eta$ (i.e., $F^{\mathrm{non-}\eta}_{\mathrm{bkg}}$) are described

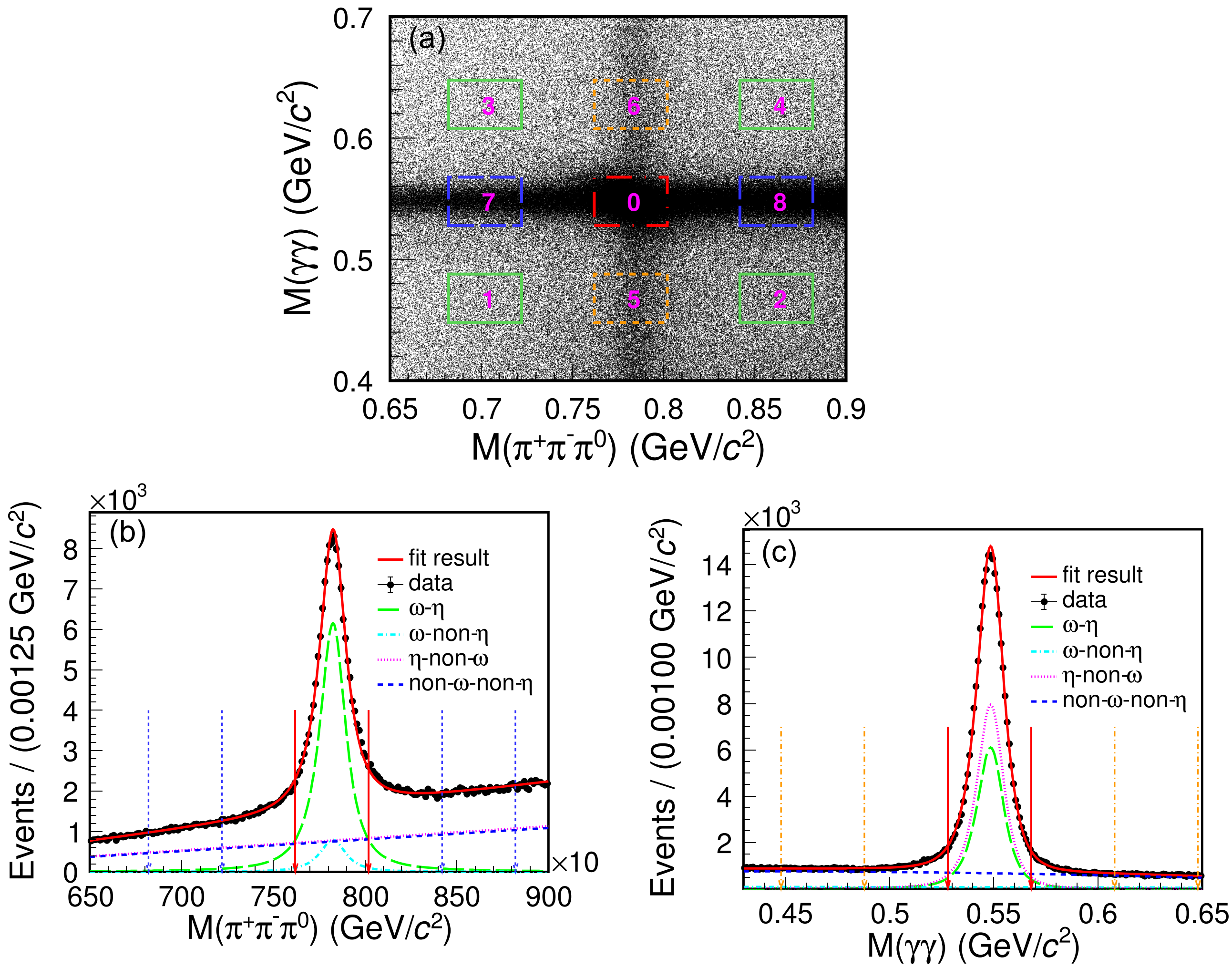


FIG. 1. (a) The distribution of $M(\pi^+\pi^-\pi^0)$ versus $M(\gamma\gamma)$ of the accepted candidates for $J/\psi \to K^+K^-\pi^+\pi^-\pi^0\gamma\gamma$ in data. Projections of the 2D fit on (b) $M(\pi^+\pi^-\pi^0)$ and (c) $M(\gamma\gamma)$ of the accepted candidates for $J/\psi \to K^+K^-\pi^+\pi^-\pi^0\gamma\gamma$. The dots with error bars are data and the red solid lines represent the fit result. The green dash lines denote the $\omega-\eta$ signal shape, the cyan dot-dashed lines represent the $\omega-$ non-$\eta$ peaking backgrounds, the pink dotted lines denote the $\eta$- non-$\omega$ peaking backgrounds and the blue short-dashed lines are the non-$\omega-$ non-$\eta$ peaking backgrounds. The blue short-dashed arrows and yellow dot-dashed arrows point to the sideband regions of $\omega$ and $\eta$, respectively. The red solid arrows point to the signal regions of $\omega/\eta$.

by first-order and second-order Chebyshev polynomial functions with free parameters, respectively. $N_{\mathrm{sig}}$ is the number of signal events, while $N_{\mathrm{bkg}}^{\mathrm{non}-\eta}$, $N_{\mathrm{bkg}}^{\mathrm{non}-\omega}$, and $N_{\mathrm{bkg}}^{\mathrm{non}-\omega\eta}$ represent the event numbers of the three types of backgrounds mentioned above. The projections of the 2D fit on $M(\pi^+\pi^-\pi^0)$ and $M(\gamma\gamma)$ are shown in Fig. 1. The BF of $J/\psi \to \omega K^+K^-\eta$ is calculated by

$$B(J/\psi \to \omega K^+K^-\eta) = \frac{N_{\mathrm{sig}}}{N_{J/\psi} \cdot B_{\mathrm{int}} \cdot \epsilon}, \tag{2}$$

where $\epsilon = 9.98\%$ is the detection efficiency obtained by MC simulation, $N_{J/\psi}$ is the number of $J/\psi$ events in the data sample, and $B_{\mathrm{int}}$ is the product of the BFs for $\omega \to \pi^+\pi^-\pi^0$, $\pi^0 \to \gamma\gamma$ and $\eta \to \gamma\gamma$ quoted from the PDG [25]. The signal yield from the 2D fit is $N_{\mathrm{sig}} = 116136 \pm 504$. The BF is determined to be $B(J/\psi \to \omega K^+K^-\eta) = (3.33 \pm 0.02(\mathrm{stat})) \times 10^{-4}$.

### C. Systematic uncertainties

The systematic uncertainties on the BF measurement are from tracking, PID, photon detection, the number of $J/\psi$ events, quoted BFs, the 5C kinematic fit, background rejection, the 2D fit, and MC simulation. Details are discussed below.

The systematic uncertainties associated with $\pi^\pm$ tracking and PID are evaluated using a control sample of $J/\psi \to p\bar{p}\pi^+\pi^-$. The efficiency differences between data and MC simulation for the control sample are used to reweight the signal MC sample. The systematic uncertainties of tracking and PID of two pions are both taken as 1.7%. Similarly, the systematic uncertainties of tracking and PID of two kaons ($K^{\pm}$) are assigned as 0.5% and 0.1%, respectively, using a control sample of $e^+e^- \to \pi^+\pi^- J/\psi$ with $J/\psi \to K^+K^-K^+K^-$.

The systematic uncertainty related to the photon detection is studied using a control sample of $e^+e^- \to \gamma\mu^+\mu^-$ [33]. The relative difference of 1.4% in the momentum reweighted efficiency between data and MC simulation is assigned as the systematic uncertainty.

The systematic uncertainty from the number of $J/\psi$ events is 0.4% according to Ref. [17]. The quoted BFs [25] of $\omega \to \pi^+\pi^-\pi^0$, $\pi^0 \to \gamma\gamma$, and $\eta \to \gamma\gamma$ are $(89.2 \pm 0.7)\%$, $(98.823 \pm 0.034)\%$, and $(39.36 \pm 0.18)\%$, respectively. The quadratic sum of the individual contributions, 0.9%, is assigned as the total systematic uncertainty due to the quoted BFs.

The systematic uncertainty from the kinematic fit is estimated by correcting the helix parameters of the charged tracks in the MC simulation [34]. The differences in the detection efficiencies with and without the corrections for the helix parameters, 0.8%, is the taken as the uncertainty.

The systematic uncertainty from the $\eta'$ veto is estimated by varying its veto range within $\pm 1\sigma$. The maximum change of 0.9% in BF is assigned as the systematic uncertainty.

To estimate the systematic uncertainties related to the signal shapes, an approach based on MC simulations is used. Two thousand sets of MC simulation samples, with an equivalent size as data, are generated based on the nominal fitting results. Each of them is fitted with both the nominal and alternative signal shapes. The alternative signal shape is modeled with a sum of two Johnson functions [32] and a Crystal Ball function [35]. The relative differences in the signal yields between the nominal fit and alternative are calculated. This distribution of the differences is then fitted with a Gaussian distribution. The mean values of individual Gaussian distributions, 0.5% and 0.3%, are taken as the systematic uncertainties for the $\omega$ and $\eta$ signal shapes, respectively.

To evaluate the systematic uncertainties from the background shapes, the same method as that for the signal shape is applied. The background shapes are changed from the first-order to a second-order Chebyshev polynomial function for the non-$\omega$ backgrounds, and from the second-order to a third-order Chebyshev polynomial function for the non-$\eta$ backgrounds. The systematic uncertainties due to the background shapes for non-$\omega$ and non-$\eta$ are determined to be 0.3% and 0.4%, respectively.

To take into account the difference between data and MC simulation in the invariant mass distributions of $K^+K^-$, the invariant mass spectra are divided into ten bins, and an averaged efficiency is calculated from the signal MC by weighting the efficiency obtained for each bin by the fraction of generated events for each bin; in an analogous way, the averaged efficiency is calculated for the data sample by weighting the selected events using the bin-dependent efficiency obtained from MC. The difference between the averaged efficiency for simulation and for data is taken as the systematic uncertainty of MC model.

TABLE I. Relative systematic uncertainties on the BF measurement for $J/\psi \to \omega K^+K^-\eta$.

| Source | Uncertainty (%) |
|---|---|
| $\pi^{\pm}$ tracking | 1.7 |
| $K^{\pm}$ tracking | 0.5 |
| $\pi^{\pm}$ PID | 1.7 |
| $K^{\pm}$ PID | 0.1 |
| Photon selection | 1.4 |
| Number of $J/\psi$ events | 0.4 |
| Quoted BFs | 0.9 |
| Kinematic fit | 0.8 |
| Veto of $\eta'$ | 0.9 |
| Signal shape | 0.5 |
| Background shape | 0.4 |
| MC model | 1.5 |
| Total | 3.6 |

The systematic uncertainties are summarized in Table I. Each source of systematic uncertainty is treated as an individual value and summed in quadrature.

## V. SEARCH FOR $X(1870)$ IN $J/\psi \to \omega X(1870) \to \omega K^+K^-\eta$

Furthermore, we search for the $X(1870)$ resonance in the distribution of the $K^+K^-\eta$ invariant mass, $M(K^+K^-\eta)$, based on the selected candidates for $J/\psi \to \omega K^+K^-\eta$.

### A. Background analysis

Detailed topology analysis with the inclusive MC sample within the mass range of $[1.7, 2.1]$ GeV$/c^2$ of the $K^+K^-\eta$ mass spectrum indicates that there is no peaking background with both $\omega$ and $\eta$ in the final states. To estimate the background contribution, we use a data-driven approach that utilizes 2D sideband regions of $\omega$ and $\eta$. The sideband regions of $\omega/\eta$ are defined as $0.06\ \mathrm{GeV}/c^2 < |M(\pi^+\pi^-\pi^0) - m(\omega)| < 0.1\ \mathrm{GeV}/c^2$ and $0.06\ \mathrm{GeV}/c^2 < |M(\gamma\gamma) - m(\eta)| < 0.1\ \mathrm{GeV}/c^2$, corresponding to (7–13)$\sigma$ away from the $\omega$ or $\eta$ nominal masses. In Fig. 1(a), the regions A is indicated with green solid line boxes, while the regions B is marked with yellow short-dashed line boxes and the regions C with blue dash line boxes. The number of background events in the signal region, denoted as $N_{\mathrm{bkg}}$, is estimated as $N_{\mathrm{bkg}} = 0.50N_{\mathrm{B}} + 0.53N_{\mathrm{C}} - 0.265N_{\mathrm{A}}$, where $N_{\mathrm{A}}$, $N_{\mathrm{B}}$, and $N_{\mathrm{C}}$ represent the number of events in regions A, B, and C, respectively. The normalization factors for events in the sideband regions are estimated by the 2D fit on $M(\pi^+\pi^-\pi^0)$ and $M(\gamma\gamma)$ of the accepted candidates for $J/\psi \to K^+K^-\pi^+\pi^-\pi^0\gamma\gamma$ in data. The fitting model for the 2D fit and the fit results are as described above. The background fraction is estimated to be 28.5%.

### B. Upper limit of the branching fraction for $X(1870)$

To search for $X(1870)$ via the decay $J/\psi \to \omega X(1870) \to \omega K^+K^-\eta$, the maximum likelihood fit is performed to the $M(K^+K^-\eta)$ distribution of the accepted candidates for $J/\psi \to \omega K^+K^-\eta$. In the fit, it is assumed that there is no interference between the $X(1870)$ and non-$X(1870)$ components. The signal shape is described by a Breit-Wigner function defined as

$$f(s) = |\mathrm{BW}(s)|^2 = \left|\frac{1}{M_\mathrm{R}^2 - s - iM_\mathrm{R}\Gamma_\mathrm{R}}\right|^2, \qquad (3)$$

where $M_\mathrm{R}$ and $\Gamma_\mathrm{R}$ are the mass and width of the $X(1870)$. The width of the Breit-Wigner function is fixed to 0.057 GeV$/c^2$ and the mass is fixed to 1.8773 GeV$/c^2$ [9]. $\sqrt{s}$ is the $K^+K^-\eta$ invariant mass. The background contributions are estimated with the $\omega/\eta$ 2D sidebands. The nonresonant contribution is described by a free third-order Chebyshev polynomial function. The full range of the $M(K^+K^-\eta)$ distribution and the fit result are shown in Fig. 2, where the cyan line represents the fitted $X(1870)$ signal. Since no $X(1870)$ signal is observed, the upper limit on the number of $X(1870)$ signal events is determined at the 90% confidence level (CL). The details are described in the next section.

### C. Systematic uncertainties

In the search for $J/\psi \to \omega X(1870) \to \omega K^+K^-\eta$, the systematic uncertainties are categorized into additive and multiplicative uncertainties. The additive uncertainties originate from the fit to extract the signal yield. The uncertainty in the signal shape is studied by changing the Breit-Wigner function to the MC simulated shape. The systematic uncertainty related to the width and mass of $X(1870)$ is estimated by varying the nominal mass and width by $\pm 1\sigma$ [9]. To account for the systematic uncertainty arising from the 2D sideband backgrounds, the number of events in the 2D sideband backgrounds is varied within $\pm 1\sigma$ and the sideband shape is varied by shifting the sideband ranges within $\pm 1\sigma$. The systematic uncertainty from the nonpeaking background is examined with an alternative fit with a second-order Chebyshev polynomial function. The resulting upper limits for each case are determined and the maximum value is taken as the upper limit.

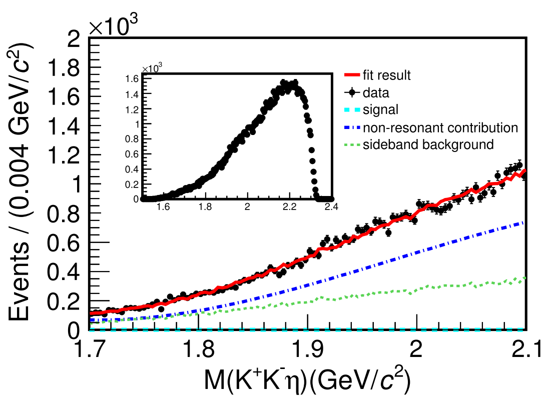


FIG. 2. The fit to the $M(K^+K^-\eta)$ distribution of the accepted candidates for $J/\psi \to \omega K^+K^-\eta$. The inset plot shows the full range of the $M(K^+K^-\eta)$ distribution. The dots with error bars are data and the red solid line represents the fit result. The cyan short-dashed line represents the fitted signal shape, the green dotted line denotes the 2D $\omega/\eta$ sideband background from data and the blue dot-dashed line represents other nonpeaking backgrounds.

The multiplicative uncertainties are associated with the efficiencies, and will affect the BF calculation. The systematic uncertainties from the tracking and PID, photon selection, the number of $J/\psi$ events, and the quoted BFs are the same as those mentioned above.

The systematic uncertainty associated with the $\omega$ or $\eta$ signal region selection is estimated by varying the $\omega$ and $\eta$ signal regions. The relative differences in efficiencies between data and MC simulation, 1.2% for $\omega$ and 1.6% for $\eta$, are taken as the systematic uncertainties.

The systematic uncertainty in the quantum numbers of the $X(1870)$ is evaluated by assuming that it as a pseudoscalar meson. The resulting 7.7% change in efficiency is considered as the systematic uncertainty.

A difference of 1.4% in efficiency with and without correcting the helix parameters in the 5C kinematic fit is taken as the systematic uncertainty due to the kinematic fit.

The systematic uncertainty associated with the $\eta'$ veto is studied by varying the $\eta'$ veto range within $\pm 1\sigma$ of its fitted resolution. The maximum difference of 1.0% in the BF is take as the uncertainty.

The multiplicative uncertainties on the BF measurement for $J/\psi \to \omega X(1870) \to \omega K^+K^-\eta$ are summarized in Table II. The total multiplicative systematic uncertainty is obtained by summing the individual contributions in quadrature.

To incorporate the multiplicative systematic uncertainties in the calculation of the upper limit, the likelihood distribution is convolved by a Gaussian function with a

TABLE II. Multiplicative uncertainties for the upper limit on the BF measurement for $J/\psi \to \omega X(1870) \to \omega K^+K^-\eta$.

| Source | Uncertainty (%) |
| --- | --- |
| $\pi^\pm$ tracking | 1.7 |
| $K^\pm$ tracking | 0.5 |
| $\pi^\pm$ PID | 1.7 |
| $K^\pm$ PID | 0.1 |
| Photon selection | 1.4 |
| Number of $J/\psi$ events | 0.4 |
| Quoted BFs | 0.9 |
| Kinematic fit | 1.4 |
| Veto of $\eta'$ | 1.0 |
| $\omega$ signal region | 1.2 |
| $\eta$ signal region | 1.6 |
| Quantum number of $X(1870)$ | 7.7 |
| Total | 8.7 |

mean of zero and a width equal to $\sigma_\epsilon$, as described in Refs. [36–39], with

$$L'(B) \propto \int_0^1 L\left(B\frac{\epsilon}{\epsilon_0}\right) e^{\frac{-(\epsilon-\epsilon_0)^2}{2\sigma_\epsilon^2}} d\epsilon, \qquad (4)$$

where $L(B)$ is the likelihood distribution as a function of the yield $n$, $\epsilon_0$ is the detection efficiency, and $\sigma_\epsilon$ is the multiplicative systematic uncertainty. The upper limit on the BF at the 90% C. L., $B_{\rm sig}^{\rm UL}$, is obtained by integrating the likelihood function to 90% of its physical region. Finally, with the detection efficiency ($\epsilon'$) of 7.02% obtained from MC simulation, the upper limit on the BF of the signal decay at the 90% CL is set to be $9.55 \times 10^{-7}$.

## VI. SUMMARY

Based on the sample of $(10087 \pm 44) \times 10^6$ $J/\psi$ events collected from the BESIII detector, the BF of the decay $J/\psi \to \omega K^+K^-\eta$ is measured to be $(3.33 \pm 0.02(\mathrm{stat}) \pm 0.12(\mathrm{syst})) \times 10^{-4}$ for the first time. No significant $J/\psi \to \omega X(1870) \to K^+K^-\eta$ signal is observed. The upper limit on the product BF of the decay $J/\psi \to \omega X(1870) \to \omega K^+K^-\eta$ at the 90% CL is determined to be $9.55 \times 10^{-7}$ for the first time. In Ref. [9], the $X(1870)$ resonance had a clear signal in the $\pi^+\pi^-\eta$ invariant mass spectrum. However, there is no evidence of $X(1870)$ in the $K^+K^-\eta$ invariant mass spectrum. The product BF (or the upper limit on the product BF) of the two decay modes of $X(1870)$ differs by 3 orders of magnitude. The probability of the $X(1870)$ decaying via the $K^+K^-\eta$ decay mode is lower compared to its decay via the $\pi^+\pi^-\eta$ decay mode. This suggests that the $X(1870)$ may have a limited $s$-quark content. To understand the nature of $X(1870)$, it is critical to measure its spin and parity and to search for it in more decay modes with higher statistics of $J/\psi$ data samples in the future.


## ACKNOWLEDGMENTS

The BESIII Collaboration thanks the staff of BEPCII and the IHEP computing center for their strong support. This work is supported in part by National Key R&D Program of China under Contracts No. 2020YFA0406300, No. 2020YFA0406400, No. 2023YFA1606000; National Natural Science Foundation of China (NSFC) under Contracts No. 11635010, No. 11735014, No. 11935015, No. 11935016, No. 11935018, No. 12025502, No. 12035009, No. 12035013, No. 12061131003, No. 12192260, No. 12192261, No. 12192262, No. 12192263, No. 12192264, No. 12192265, No. 12221005, No. 12225509, No. 12235017, No. 12342502, No. 12361141819, No. U23B2070; the Chinese Academy of Sciences (CAS) Large-Scale Scientific Facility Program; the CAS Center for Excellence in Particle Physics (CCEPP); Joint Large-Scale Scientific Facility Funds of the NSFC and CAS under Contract No. U1832207; 100 Talents Program of CAS; The Institute of Nuclear and Particle Physics (INPAC) and Shanghai Key Laboratory for Particle Physics and Cosmology; German Research Foundation DFG under Contracts No. 455635585, No. FOR5327, No. GRK 2149; Istituto Nazionale di Fisica Nucleare, Italy; Ministry of Development of Turkey under Contract No. DPT2006K-120470; National Research Foundation of Korea under Contract No. NRF-2022R1A2C1092335; National Science and Technology fund of Mongolia; National Science Research and Innovation Fund (NSRF) via the Program Management Unit for Human Resources & Institutional Development, Research and Innovation of Thailand under Contract No. B16F640076; Polish National Science Centre under Contract No. 2019/35/O/ST2/02907; The Swedish Research Council; U.S. Department of Energy under Contract No. DE-FG02-05ER41374.



[1] J. Z. Bai *et al.* (BES Collaboration), Phys. Rev. Lett. **91**, 022001 (2003).
[2] J. P. Alexander *et al.* (CLEO Collaboration), Phys. Rev. D **82**, 092002 (2010).
[3] M. Ablikim *et al.* (BESIII Collaboration), Phys. Rev. Lett. **108**, 112003 (2012).
[4] M. Ablikim *et al.* (BES Collaboration), Phys. Rev. Lett. **95**, 262001 (2005).
[5] M. Ablikim *et al.* (BESIII Collaboration), Phys. Rev. Lett. **106**, 072002 (2011).
[6] M. Ablikim *et al.* (BESIII Collaboration), Phys. Rev. Lett. **115**, 091803 (2015).
[7] M. Ablikim *et al.* (BESIII Collaboration), Phys. Rev. D **99**, 071101 (2019).
[8] M. Ablikim *et al.* (BESIII Collaboration), Phys. Rev. D **87**, 032008 (2013).
[9] M. Ablikim *et al.* (BESIII Collaboration), Phys. Rev. Lett. **107**, 182001 (2011).
[10] M. Ablikim *et al.* (BESIII Collaboration), Nucl. Instrum. Methods Phys. Res., Sect. A **614**, 345 (2010).
[11] M. Ablikim *et al.* (BESIII Collaboration), Chin. Phys. C **44**, 040001 (2020).
[12] K. X. Huang, Z. J. Li, Z. Qian, J. Zhu, H. Y. Li, Y. M. Zhang *et al.*, Nucl. Sci. Tech. **33**, 142 (2022).
[13] C. Yu *et al.*, BEPCII performance and beam dynamics studies on luminosity, in *7th International Particle Accelerator Conference* (2016), p. TUYA01, https://accelconf.web.cern.ch/ipac2016/doi/JACoW-IPAC2016-TUYA01.html.

[14] X. Li *et al.*, Radiat. Detect. Technol. Methods **1**, 13 (2017).
[15] Y. X. Guo *et al.*, Radiat. Detect. Technol. Methods **1**, 15 (2017).
[16] P. Cao *et al.*, Nucl. Instrum. Methods Phys. Res., Sect. A **953**, 163053 (2020).
[17] M. Ablikim *et al.* (BESIII Collaboration), Chin. Phys. C **46**, 074001 (2022).
[18] S. Agostinelli *et al.* (GEANT4 Collaboration), Nucl. Instrum. Methods Phys. Res., Sect. A **506**, 250 (2003).
[19] Z. Y. Deng *et al.*, Chin. Phys. C **30**, 371 (2006), http://cpc.ihep.ac.cn/article/id/283d17c0-e8fa-4ad7-bfe3-92095466def1.
[20] Y. T. Liang, B. Zhu, Z. Y. You *et al.*, Nucl. Instrum. Methods Phys. Res., Sect. A **603**, 325 (2009).
[21] Z. Y. You, Y. T. Liang, and Y. J. Mao, Chin. Phys. C **32**, 572 (2008).
[22] S. Jadach, B. F. L. Ward, and Z. Was, Comput. Phys. Commun. **130**, 260 (2000).
[23] S. Jadach, B. F. L. Ward, and Z. Was, Phys. Rev. D **63**, 113009 (2001).
[24] D. J. Lange, Nucl. Instrum. Methods Phys. Res., Sect. A **462**, 152 (2001).
[25] R. L. Workman *et al.* (Particle Data Group), Prog. Theor. Exp. Phys. **2022**, 083C01 (2022).
[26] J. C. Chen, G. S. Huang, X. R. Qi, D. H. Zhang, and Y. S. Zhu, Phys. Rev. D **62**, 034003 (2000).
[27] E. Barberio, B. van Eijk, and Z. Was, Comput. Phys. Commun. **66**, 115 (1991).
[28] R. G. Ping, Chin. Phys. C **32**, 599 (2008).
[29] L. Yan *et al.*, Chin. Phys. C **34**, 204–209 (2010).
[30] G. Punzi, PHYSTAT2003, SLAC, Stanford, California (2003), pp. 79–83, arXiv:physics/0308063.
[31] X. Y. Zhou, S. Du, G. Li, and C. Shen, Comput. Phys. Commun. **258**, 107540 (2021).
[32] N. L. Johnson, Biometrika **36**, 149 (1949).
[33] M. Ablikim *et al.* (BESIII Collaboration), Phys. Rev. D **108**, 092002 (2023).
[34] M. Ablikim *et al.* (BESIII Collaboration), Phys. Rev. D **87**, 012002 (2013).
[35] S. Das, arXiv:1603.08591.
[36] G. J. Feldman and R. D. Cousins, Phys. Rev. D **57**, 3873 (1998).
[37] K. Stenson, arXiv:physics/0605236.
[38] M. Ablikim *et al.* (BESIII Collaboration), J. High Energy Phys. 05 (2024) 141.
[39] X. X. Liu, X. R. Lü, and Y. S. Zhu, Chin. Phys. C **39**, 103001 (2015).

M. Ablikim,[1] M. N. Achasov,[4,c] P. Adlarson,[76] O. Afedulidis,[3] X. C. Ai,[81] R. Aliberti,[35] A. Amoroso,[75a,75c] Q. An,[72,58,a] Y. Bai,[57] O. Bakina,[36] I. Balossino,[29a] Y. Ban,[46,h] H.-R. Bao,[64] V. Batozskaya,[1,44] K. Begzsuren,[32] N. Berger,[35] M. Berlowski,[44] M. Bertani,[28a] D. Bettoni,[29a] F. Bianchi,[75a,75c] E. Bianco,[75a,75c] A. Bortone,[75a,75c] I. Boyko,[36] R. A. Briere,[5] A. Brueggemann,[69] H. Cai,[77] X. Cai,[1,58] A. Calcaterra,[28a] G. F. Cao,[1,64] N. Cao,[1,64] S. A. Cetin,[62a] X. Y. Chai,[46,h] J. F. Chang,[1,58] G. R. Che,[43] G. Chelkov,[36,b] C. Chen,[43] C. H. Chen,[9] Chao Chen,[55] G. Chen,[1] H. S. Chen,[1,64] H. Y. Chen,[20] M. L. Chen,[1,58,64] S. J. Chen,[42] S. L. Chen,[45] S. M. Chen,[61] T. Chen,[1,64] X. R. Chen,[31,64] X. T. Chen,[1,64] Y. B. Chen,[1,58] Y. Q. Chen,[34] Z. J. Chen,[25,i] Z. Y. Chen,[1,64] S. K. Choi,[10] G. Cibinetto,[29a] F. Cossio,[75c] J. J. Cui,[50] H. L. Dai,[1,58] J. P. Dai,[79] A. Dbeyssi,[18] R. E. de Boer,[3] D. Dedovich,[36] C. Q. Deng,[73] Z. Y. Deng,[1] A. Denig,[35] I. Denysenko,[36] M. Destefanis,[75a,75c] F. De Mori,[75a,75c] B. Ding,[67,1] X. X. Ding,[46,h] Y. Ding,[34] Y. Ding,[40] J. Dong,[1,58] L. Y. Dong,[1,64] M. Y. Dong,[1,58,64] X. Dong,[77] M. C. Du,[1] S. X. Du,[81] Y. Y. Duan,[55] Z. H. Duan,[42] P. Egorov,[36,b] Y. H. Fan,[45] J. Fang,[59] J. Fang,[1,58] S. S. Fang,[1,64] W. X. Fang,[1] Y. Fang,[1] Y. Q. Fang,[1,58] R. Farinelli,[29a] L. Fava,[75b,75c] F. Feldbauer,[3] G. Felici,[28a] C. Q. Feng,[72,58] J. H. Feng,[59] Y. T. Feng,[72,58] M. Fritsch,[3] C. D. Fu,[1] J. L. Fu,[64] Y. W. Fu,[1,64] H. Gao,[64] X. B. Gao,[41] Y. N. Gao,[46,h] Yang Gao,[72,58] S. Garbolino,[75c] I. Garzia,[29a,29b] L. Ge,[81] P. T. Ge,[19] Z. W. Ge,[42] C. Geng,[59] E. M. Gersabeck,[68] A. Gilman,[70] K. Goetzen,[13] L. Gong,[40] W. X. Gong,[1,58] W. Gradl,[35] S. Gramigna,[29a,29b] M. Greco,[75a,75c] M. H. Gu,[1,58] Y. T. Gu,[15] C. Y. Guan,[1,64] A. Q. Guo,[31,64] L. B. Guo,[41] M. J. Guo,[50] R. P. Guo,[49] Y. P. Guo,[12,g] A. Guskov,[36,b] J. Gutierrez,[27] K. L. Han,[64] T. T. Han,[1] F. Hanisch,[3] X. Q. Hao,[19] F. A. Harris,[66] K. K. He,[55] K. L. He,[1,64] F. H. Heinsius,[3] C. H. Heinz,[35] Y. K. Heng,[1,58,64] C. Herold,[60] T. Holtmann,[3] P. C. Hong,[34] G. Y. Hou,[1,64] X. T. Hou,[1,64] Y. R. Hou,[64] Z. L. Hou,[1] B. Y. Hu,[59] H. M. Hu,[1,64] J. F. Hu,[56,j] S. L. Hu,[12,g] T. Hu,[1,58,64] Y. Hu,[1] G. S. Huang,[72,58] K. X. Huang,[59] L. Q. Huang,[31,64] X. T. Huang,[50] Y. P. Huang,[1] Y. S. Huang,[59] T. Hussain,[74] F. Hölzken,[3] N. Hüsken,[35] N. in der Wiesche,[69] J. Jackson,[27] S. Janchiv,[32] J. H. Jeong,[10] Q. Ji,[1] Q. P. Ji,[19] W. Ji,[1,64] X. B. Ji,[1,64] X. L. Ji,[1,58] Y. Y. Ji,[50] X. Q. Jia,[50] Z. K. Jia,[72,58] D. Jiang,[1,64] H. B. Jiang,[77] P. C. Jiang,[46,h] S. S. Jiang,[39] T. J. Jiang,[16] X. S. Jiang,[1,58,64] Y. Jiang,[64] J. B. Jiao,[50] J. K. Jiao,[34] Z. Jiao,[23] S. Jin,[42] Y. Jin,[67] M. Q. Jing,[1,64] X. M. Jing,[64] T. Johansson,[76] S. Kabana,[33] N. Kalantar-Nayestanaki,[65] X. L. Kang,[9] X. S. Kang,[40] M. Kavatsyuk,[65] B. C. Ke,[81] V. Khachatryan,[27] A. Khoukaz,[69] R. Kiuchi,[1] O. B. Kolcu,[62a] B. Kopf,[3] M. Kuessner,[3] X. Kui,[1,64] N. Kumar,[26] A. Kupsc,[44,76] W. Kühn,[37] J. J. Lane,[68] L. Lavezzi,[75a,75c] T. T. Lei,[72,58] Z. H. Lei,[72,58] M. Lellmann,[35] T. Lenz,[35] C. Li,[47] C. Li,[43] C. H. Li,[39] Cheng Li,[72,58] D. M. Li,[81] F. Li,[1,58] G. Li,[1] H. B. Li,[1,64] H. J. Li,[19] H. N. Li,[56,j] Hui Li,[43] J. R. Li,[61] J. S. Li,[59] K. Li,[1] K. L. Li,[19] L. J. Li,[1,64] L. K. Li,[1] Lei Li,[48] M. H. Li,[43] P. R. Li,[38,k,l] Q. M. Li,[1,64] Q. X. Li,[50] R. Li,[17,31] S. X. Li,[12] T. Li,[50] W. D. Li,[1,64] W. G. Li,[1,a] X. Li,[1,64] X. H. Li,[72,58] X. L. Li,[50] X. Y. Li,[1,64] X. Z. Li,[59] Y. G. Li,[46,h] Z. J. Li,[59]

Z. Y. Li,[79] C. Liang,[42] H. Liang,[1,64] H. Liang,[72,58] Y. F. Liang,[54] Y. T. Liang,[31,64] G. R. Liao,[14] Y. P. Liao,[1,64] J. Libby,[26] A. Limphirat,[60] C. C. Lin,[55] D. X. Lin,[31,64] T. Lin,[1] B. J. Liu,[1] B. X. Liu,[77] C. Liu,[34] C. X. Liu,[1] F. Liu,[1] F. H. Liu,[53] Feng Liu,[6] G. M. Liu,[56,j] H. Liu,[38,k,l] H. B. Liu,[15] H. H. Liu,[1] H. M. Liu,[1,64] Huihui Liu,[21] J. B. Liu,[72,58] J. Y. Liu,[1,64] K. Liu,[38,k,l] K. Y. Liu,[40] Ke Liu,[22] L. Liu,[72,58] L. C. Liu,[43] Lu Liu,[43] M. H. Liu,[12,g] P. L. Liu,[1] Q. Liu,[64] S. B. Liu,[72,58] T. Liu,[12,g] W. K. Liu,[43] W. M. Liu,[72,58] X. Liu,[38,k,l] X. Liu,[39] Y. Liu,[81] Y. Liu,[38,k,l] Y. B. Liu,[43] Z. A. Liu,[1,58,64] Z. D. Liu,[9] Z. Q. Liu,[50] X. C. Lou,[1,58,64] F. X. Lu,[59] H. J. Lu,[23] J. G. Lu,[1,58] X. L. Lu,[1] Y. Lu,[7] Y. P. Lu,[1,58] Z. H. Lu,[1,64] C. L. Luo,[41] J. R. Luo,[59] M. X. Luo,[80] T. Luo,[12,g] X. L. Luo,[1,58] X. R. Lyu,[64] Y. F. Lyu,[43] F. C. Ma,[40] H. Ma,[79] H. L. Ma,[1] J. L. Ma,[1,64] L. L. Ma,[50] L. R. Ma,[67] M. M. Ma,[1,64] Q. M. Ma,[1] R. Q. Ma,[1,64] T. Ma,[72,58] X. T. Ma,[1,64] X. Y. Ma,[1,58] Y. M. Ma,[31] F. E. Maas,[18] I. MacKay,[70] M. Maggiora,[75a,75c] S. Malde,[70] Y. J. Mao,[46,h] Z. P. Mao,[1] S. Marcello,[75a,75c] Z. X. Meng,[67] J. G. Messchendorp,[13,65] G. Mezzadri,[29a] H. Miao,[1,64] T. J. Min,[42] R. E. Mitchell,[27] X. H. Mo,[1,58,64] B. Moses,[27] N. Yu. Muchnoi,[4,c] J. Muskalla,[35] Y. Nefedov,[36] F. Nerling,[18,e] L. S. Nie,[20] I. B. Nikolaev,[4,c] Z. Ning,[1,58] S. Nisar,[11,m] Q. L. Niu,[38,k,l] W. D. Niu,[55] Y. Niu,[50] S. L. Olsen,[64] S. L. Olsen,[10,64] Q. Ouyang,[1,58,64] S. Pacetti,[28b,28c] X. Pan,[55] Y. Pan,[57] A. Pathak,[34] Y. P. Pei,[72,58] M. Pelizaeus,[3] H. P. Peng,[72,58] Y. Y. Peng,[38,k,l] K. Peters,[13,e] J. L. Ping,[41] R. G. Ping,[1,64] S. Plura,[35] V. Prasad,[33] F. Z. Qi,[1] H. Qi,[72,58] H. R. Qi,[61] M. Qi,[42] T. Y. Qi,[12,g] S. Qian,[1,58] W. B. Qian,[64] C. F. Qiao,[64] X. K. Qiao,[81] J. J. Qin,[73] L. Q. Qin,[14] L. Y. Qin,[72,58] X. P. Qin,[12,g] X. S. Qin,[50] Z. H. Qin,[1,58] J. F. Qiu,[1] Z. H. Qu,[73] C. F. Redmer,[35] K. J. Ren,[39] A. Rivetti,[75c] M. Rolo,[75c] G. Rong,[1,64] Ch. Rosner,[18] S. N. Ruan,[43] N. Salone,[44] A. Sarantsev,[36,d] Y. Schelhaas,[35] K. Schoenning,[76] M. Scodeggio,[29a] K. Y. Shan,[12,g] W. Shan,[24] X. Y. Shan,[72,58] Z. J. Shang,[38,k,l] J. F. Shangguan,[16] L. G. Shao,[1,64] M. Shao,[72,58] C. P. Shen,[12,g] H. F. Shen,[1,8] W. H. Shen,[64] X. Y. Shen,[1,64] B. A. Shi,[64] H. Shi,[72,58] H. C. Shi,[72,58] J. L. Shi,[12,g] J. Y. Shi,[1] Q. Q. Shi,[55] S. Y. Shi,[73] X. Shi,[1,58] J. J. Song,[19] T. Z. Song,[59] W. M. Song,[34,1] Y. J. Song,[12,g] Y. X. Song,[46,h,n] S. Sosio,[75a,75c] S. Spataro,[75a,75c] F. Stieler,[35] S. S. Su,[40] Y. J. Su,[64] G. B. Sun,[77] G. X. Sun,[1] H. Sun,[64] H. K. Sun,[1] J. F. Sun,[19] K. Sun,[61] L. Sun,[77] S. S. Sun,[1,64] T. Sun,[51,f] W. Y. Sun,[34] Y. Sun,[9] Y. J. Sun,[72,58] Y. Z. Sun,[1] Z. Q. Sun,[1,64] Z. T. Sun,[50] C. J. Tang,[54] G. Y. Tang,[1] J. Tang,[59] M. Tang,[72,58] Y. A. Tang,[77] L. Y. Tao,[73] Q. T. Tao,[25,i] M. Tat,[70] J. X. Teng,[72,58] V. Thoren,[76] W. H. Tian,[59] Y. Tian,[31,64] Z. F. Tian,[77] I. Uman,[62b] Y. Wan,[55] S. J. Wang,[50] B. Wang,[1] B. L. Wang,[64] Bo Wang,[72,58] D. Y. Wang,[46,h] F. Wang,[73] H. J. Wang,[38,k,l] J. J. Wang,[77] J. P. Wang,[50] K. Wang,[1,58] L. L. Wang,[1] M. Wang,[50] N. Y. Wang,[64] S. Wang,[38,k,l] S. Wang,[12,g] T. Wang,[12,g] T. J. Wang,[43] W. Wang,[73] W. Wang,[59] W. P. Wang,[35,58,72,o] X. Wang,[46,h] X. F. Wang,[38,k,l] X. J. Wang,[39] X. L. Wang,[12,g] X. N. Wang,[1] Y. Wang,[61] Y. D. Wang,[45] Y. F. Wang,[1,58,64] Y. L. Wang,[19] Y. N. Wang,[45] Y. Q. Wang,[1] Yaqian Wang,[17] Yi Wang,[61] Z. Wang,[1,58] Z. L. Wang,[73] Z. Y. Wang,[1,64] Ziyi Wang,[64] D. H. Wei,[14] F. Weidner,[69] S. P. Wen,[1] Y. R. Wen,[39] U. Wiedner,[3] G. Wilkinson,[70] M. Wolke,[76] L. Wollenberg,[3] C. Wu,[39] J. F. Wu,[1,8] L. H. Wu,[1] L. J. Wu,[1,64] X. Wu,[12,g] X. H. Wu,[34] Y. Wu,[72,58] Y. H. Wu,[55] Y. J. Wu,[31] Z. Wu,[1,58] L. Xia,[72,58] X. M. Xian,[39] B. H. Xiang,[1,64] T. Xiang,[46,h] D. Xiao,[38,k,l] G. Y. Xiao,[42] S. Y. Xiao,[1] Y. L. Xiao,[12,g] Z. J. Xiao,[41] C. Xie,[42] X. H. Xie,[46,h] Y. Xie,[50] Y. G. Xie,[1,58] Y. H. Xie,[6] Z. P. Xie,[72,58] T. Y. Xing,[1,64] C. F. Xu,[1,64] C. J. Xu,[59] G. F. Xu,[1] H. Y. Xu,[67,2,p] M. Xu,[72,58] Q. J. Xu,[16] Q. N. Xu,[30] W. Xu,[1] W. L. Xu,[67] X. P. Xu,[55] Y. Xu,[40] Y. C. Xu,[78] Z. S. Xu,[64] F. Yan,[12,g] L. Yan,[12,g] W. B. Yan,[72,58] W. C. Yan,[81] X. Q. Yan,[1,64] H. J. Yang,[51,f] H. L. Yang,[34] H. X. Yang,[1] T. Yang,[1] Y. Yang,[12,g] Y. F. Yang,[43] Y. F. Yang,[1,64] Y. X. Yang,[1,64] Z. W. Yang,[38,k,l] Z. P. Yao,[50] M. Ye,[1,58] M. H. Ye,[8] J. H. Yin,[1] Junhao Yin,[43] Z. Y. You,[59] B. X. Yu,[1,58,64] C. X. Yu,[43] G. Yu,[1,64] J. S. Yu,[25,i] M. C. Yu,[40] T. Yu,[73] X. D. Yu,[46,h] Y. C. Yu,[81] C. Z. Yuan,[1,64] J. Yuan,[34] J. Yuan,[45] L. Yuan,[2] S. C. Yuan,[1,64] Y. Yuan,[1,64] Z. Y. Yuan,[59] C. X. Yue,[39] A. A. Zafar,[74] F. R. Zeng,[50] S. H. Zeng,[63a,63b,63c,63d] X. Zeng,[12,g] Y. Zeng,[25,i] Y. J. Zeng,[1,64] Y. J. Zeng,[59] X. Y. Zhai,[34] Y. C. Zhai,[50] Y. H. Zhan,[59] A. Q. Zhang,[1,64] B. L. Zhang,[1,64] B. X. Zhang,[1] D. H. Zhang,[43] G. Y. Zhang,[19] H. Zhang,[81] H. Zhang,[72,58] H. C. Zhang,[1,58,64] H. H. Zhang,[34] H. H. Zhang,[59] H. Q. Zhang,[1,58,64] H. R. Zhang,[72,58] H. Y. Zhang,[1,58] J. Zhang,[81] J. Zhang,[59] J. J. Zhang,[52] J. L. Zhang,[20] J. Q. Zhang,[41] J. S. Zhang,[12,g] J. W. Zhang,[1,58,64] J. X. Zhang,[38,k,l] J. Y. Zhang,[1] J. Z. Zhang,[1,64] Jianyu Zhang,[64] L. M. Zhang,[61] Lei Zhang,[42] P. Zhang,[1,64] Q. Y. Zhang,[34] R. Y. Zhang,[38,k,l] S. H. Zhang,[1,64] Shulei Zhang,[25,i] X. M. Zhang,[1] X. Y. Zhang,[40] X. Y. Zhang,[50] Y. Zhang,[73] Y. Zhang,[1] Y. T. Zhang,[81] Y. H. Zhang,[1,58] Y. M. Zhang,[39] Yan Zhang,[72,58] Z. D. Zhang,[1] Z. H. Zhang,[1] Z. L. Zhang,[34] Z. Y. Zhang,[43] Z. Y. Zhang,[77] Z. Z. Zhang,[45] G. Zhao,[1] J. Y. Zhao,[1,64] J. Z. Zhao,[1,58] L. Zhao,[1] Lei Zhao,[72,58] M. G. Zhao,[43] N. Zhao,[79] R. P. Zhao,[64] S. J. Zhao,[81] Y. B. Zhao,[1,58] Y. X. Zhao,[31,64] Z. G. Zhao,[72,58] A. Zhemchugov,[36,b] B. Zheng,[73] B. M. Zheng,[34] J. P. Zheng,[1,58] W. J. Zheng,[1,64] Y. H. Zheng,[64] B. Zhong,[41] X. Zhong,[59] H. Zhou,[50] J. Y. Zhou,[34] L. P. Zhou,[1,64] S. Zhou,[6] X. Zhou,[77] X. K. Zhou,[6] X. R. Zhou,[72,58] X. Y. Zhou,[39] Y. Z. Zhou,[12,g] Z. C. Zhou,[20] A. N. Zhu,[64] J. Zhu,[43] K. Zhu,[1] K. J. Zhu,[1,58,64] K. S. Zhu,[12,g] L. Zhu,[34] L. X. Zhu,[64] S. H. Zhu,[71] T. J. Zhu,[12,g] W. D. Zhu,[41] Y. C. Zhu,[72,58] Z. A. Zhu,[1,64] J. H. Zou,[1] and J. Zu[72,58]

(BESIII Collaboration)

[1]*Institute of High Energy Physics, Beijing 100049, People's Republic of China*
[2]*Beihang University, Beijing 100191, People's Republic of China*
[3]*Bochum Ruhr-University, D-44780 Bochum, Germany*
[4]*Budker Institute of Nuclear Physics SB RAS (BINP), Novosibirsk 630090, Russia*
[5]*Carnegie Mellon University, Pittsburgh, Pennsylvania 15213, USA*
[6]*Central China Normal University, Wuhan 430079, People's Republic of China*
[7]*Central South University, Changsha 410083, People's Republic of China*
[8]*China Center of Advanced Science and Technology, Beijing 100190, People's Republic of China*
[9]*China University of Geosciences, Wuhan 430074, People's Republic of China*
[10]*Chung-Ang University, Seoul, 06974, Republic of Korea*
[11]*COMSATS University Islamabad, Lahore Campus, Defence Road, Off Raiwind Road, 54000 Lahore, Pakistan*
[12]*Fudan University, Shanghai 200433, People's Republic of China*
[13]*GSI Helmholtzcentre for Heavy Ion Research GmbH, D-64291 Darmstadt, Germany*
[14]*Guangxi Normal University, Guilin 541004, People's Republic of China*
[15]*Guangxi University, Nanning 530004, People's Republic of China*
[16]*Hangzhou Normal University, Hangzhou 310036, People's Republic of China*
[17]*Hebei University, Baoding 071002, People's Republic of China*
[18]*Helmholtz Institute Mainz, Staudinger Weg 18, D-55099 Mainz, Germany*
[19]*Henan Normal University, Xinxiang 453007, People's Republic of China*
[20]*Henan University, Kaifeng 475004, People's Republic of China*
[21]*Henan University of Science and Technology, Luoyang 471003, People's Republic of China*
[22]*Henan University of Technology, Zhengzhou 450001, People's Republic of China*
[23]*Huangshan College, Huangshan 245000, People's Republic of China*
[24]*Hunan Normal University, Changsha 410081, People's Republic of China*
[25]*Hunan University, Changsha 410082, People's Republic of China*
[26]*Indian Institute of Technology Madras, Chennai 600036, India*
[27]*Indiana University, Bloomington, Indiana 47405, USA*
[28a]*INFN Laboratori Nazionali di Frascati, I-00044, Frascati, Italy*
[28b]*INFN Sezione di Perugia, I-06100, Perugia, Italy*
[28c]*University of Perugia, I-06100, Perugia, Italy*
[29a]*INFN Sezione di Ferrara, I-44122, Ferrara, Italy*
[29b]*University of Ferrara, I-44122, Ferrara, Italy*
[30]*Inner Mongolia University, Hohhot 010021, People's Republic of China*
[31]*Institute of Modern Physics, Lanzhou 730000, People's Republic of China*
[32]*Institute of Physics and Technology, Peace Avenue 54B, Ulaanbaatar 13330, Mongolia*
[33]*Instituto de Alta Investigación, Universidad de Tarapacá, Casilla 7D, Arica 1000000, Chile*
[34]*Jilin University, Changchun 130012, People's Republic of China*
[35]*Johannes Gutenberg University of Mainz, Johann-Joachim-Becher-Weg 45, D-55099 Mainz, Germany*
[36]*Joint Institute for Nuclear Research, 141980 Dubna, Moscow region, Russia*
[37]*Justus-Liebig-Universitaet Giessen, II. Physikalisches Institut, Heinrich-Buff-Ring 16, D-35392 Giessen, Germany*
[38]*Lanzhou University, Lanzhou 730000, People's Republic of China*
[39]*Liaoning Normal University, Dalian 116029, People's Republic of China*
[40]*Liaoning University, Shenyang 110036, People's Republic of China*
[41]*Nanjing Normal University, Nanjing 210023, People's Republic of China*
[42]*Nanjing University, Nanjing 210093, People's Republic of China*
[43]*Nankai University*, Tianjin 300071, People's Republic of China
[44]*National Centre for Nuclear Research, Warsaw 02-093, Poland*
[45]*North China Electric Power University, Beijing 102206, People's Republic of China*
[46]*Peking University, Beijing 100871, People's Republic of China*
[47]*Qufu Normal University, Qufu 273165, People's Republic of China*
[48]*Renmin University of China, Beijing 100872, People's Republic of China*
[49]*Shandong Normal University, Jinan 250014, People's Republic of China*
[50]*Shandong University, Jinan 250100, People's Republic of China*
[51]*Shanghai Jiao Tong University, Shanghai 200240, People's Republic of China*
[52]*Shanxi Normal University, Linfen 041004, People's Republic of China*
[53]*Shanxi University, Taiyuan 030006, People's Republic of China*

[54]Sichuan University, Chengdu 610064, People's Republic of China
[55]Soochow University, Suzhou 215006, People's Republic of China
[56]South China Normal University, Guangzhou 510006, People's Republic of China
[57]Southeast University, Nanjing 211100, People's Republic of China
[58]State Key Laboratory of Particle Detection and Electronics, Beijing 100049, Hefei 230026, People's Republic of China
[59]Sun Yat-Sen University, Guangzhou 510275, People's Republic of China
[60]Suranaree University of Technology, University Avenue 111, Nakhon Ratchasima 30000, Thailand
[61]Tsinghua University, Beijing 100084, People's Republic of China
[62a]Turkish Accelerator Center Particle Factory Group, Istinye University, 34010, Istanbul, Turkey
[62b]Near East University, Nicosia, North Cyprus, 99138, Mersin 10, Turkey
[63a]H H Wills Physics Laboratory, University of Bristol
[63b]Tyndall Avenue, University of Bristol
[63c]Bristol, University of Bristol
[63d]BS8 1TL, University of Bristol
[64]University of Chinese Academy of Sciences, Beijing 100049, People's Republic of China
[65]University of Groningen, NL-9747 AA Groningen, The Netherlands
[66]University of Hawaii, Honolulu, Hawaii 96822, USA
[67]University of Jinan, Jinan 250022, People's Republic of China
[68]University of Manchester, Oxford Road, Manchester, M13 9PL, United Kingdom
[69]University of Muenster, Wilhelm-Klemm-Strasse 9, 48149 Muenster, Germany
[70]University of Oxford, Keble Road, Oxford OX13RH, United Kingdom
[71]University of Science and Technology Liaoning, Anshan 114051, People's Republic of China
[72]University of Science and Technology of China, Hefei 230026, People's Republic of China
[73]University of South China, Hengyang 421001, People's Republic of China
[74]University of the Punjab, Lahore-54590, Pakistan
[75a]University of Turin and INFN, University of Turin, I-10125, Turin, Italy
[75b]University of Eastern Piedmont, I-15121, Alessandria, Italy
[75c]INFN, I-10125, Turin, Italy
[76]Uppsala University, Box 516, SE-75120 Uppsala, Sweden
[77]Wuhan University, Wuhan 430072, People's Republic of China
[78]Yantai University, Yantai 264005, People's Republic of China
[79]Yunnan University, Kunming 650500, People's Republic of China
[80]Zhejiang University, Hangzhou 310027, People's Republic of China
[81]Zhengzhou University, Zhengzhou 450001, People's Republic of China

[a]Deceased.
[b]Also at the Moscow Institute of Physics and Technology, Moscow 141700, Russia.
[c]Also at the Novosibirsk State University, Novosibirsk, 630090, Russia.
[d]Also at the NRC "Kurchatov Institute", PNPI, 188300, Gatchina, Russia.
[e]Also at Goethe University Frankfurt, 60323 Frankfurt am Main, Germany.
[f]Also at Key Laboratory for Particle Physics, Astrophysics and Cosmology, Ministry of Education; Shanghai Key Laboratory for Particle Physics and Cosmology; Institute of Nuclear and Particle Physics, Shanghai 200240, People's Republic of China.
[g]Also at Key Laboratory of Nuclear Physics and Ion-beam Application (MOE) and Institute of Modern Physics, Fudan University, Shanghai 200443, People's Republic of China.
[h]Also at State Key Laboratory of Nuclear Physics and Technology, Peking University, Beijing 100871, People's Republic of China.
[i]Also at School of Physics and Electronics, Hunan University, Changsha 410082, China.
[j]Also at Guangdong Provincial Key Laboratory of Nuclear Science, Institute of Quantum Matter, South China Normal University, Guangzhou 510006, China.
[k]Also at MOE Frontiers Science Center for Rare Isotopes, Lanzhou University, Lanzhou 730000, People's Republic of China.
[l]Also at Lanzhou Center for Theoretical Physics, Lanzhou University, Lanzhou 730000, People's Republic of China.
[m]Also at the Department of Mathematical Sciences, IBA, Karachi 75270, Pakistan.
[n]Also at Ecole Polytechnique Federale de Lausanne (EPFL), CH-1015 Lausanne, Switzerland.
[o]Also at Helmholtz Institute Mainz, Staudinger Weg 18, D-55099 Mainz, Germany.
[p]Also at School of Physics, Beihang University, Beijing 100191, China.